

Thermal excitation of plasmons for near-field thermophotovoltaics

Yu Guo, Sean Molesky, Huan Hu, Cristian L. Cortes, and Zubin Jacob

Citation: *Appl. Phys. Lett.* **105**, 073903 (2014);

View online: <https://doi.org/10.1063/1.4893665>

View Table of Contents: <http://aip.scitation.org/toc/apl/105/7>

Published by the [American Institute of Physics](#)

Articles you may be interested in

[Broadband super-Planckian thermal emission from hyperbolic metamaterials](#)

Applied Physics Letters **101**, 131106 (2012); 10.1063/1.4754616

[Near-field thermophotovoltaic energy conversion](#)

Journal of Applied Physics **100**, 063704 (2006); 10.1063/1.2234560

[Surface modes for near field thermophotovoltaics](#)

Applied Physics Letters **82**, 3544 (2003); 10.1063/1.1575936

[Near-field radiative thermal transport: From theory to experiment](#)

AIP Advances **5**, 053503 (2015); 10.1063/1.4919048

[Super-Planckian near-field thermal emission with phonon-polaritonic hyperbolic metamaterials](#)

Applied Physics Letters **102**, 131106 (2013); 10.1063/1.4800233

[Three-dimensional photonic-crystal emitter for thermal photovoltaic power generation](#)

Applied Physics Letters **83**, 380 (2003); 10.1063/1.1592614

Scilight

Sharp, quick summaries **illuminating**
the latest physics research

Sign up for **FREE!**



Thermal excitation of plasmons for near-field thermophotovoltaics

Yu Guo, Sean Molesky, Huan Hu, Cristian L. Cortes, and Zubin Jacob^{a)}

Department of Electrical and Computer Engineering, University of Alberta, Edmonton, Alberta T6G 2V4, Canada

(Received 30 May 2014; accepted 8 August 2014; published online 20 August 2014)

The traditional approaches of exciting plasmons consist of either using electrons (e.g., electron energy loss spectroscopy) or light (Kretschman and Otto geometry) while more recently plasmons have been excited even by single photons. A different approach: thermal excitation of a plasmon resonance at high temperatures using alternate plasmonic media was proposed by S. Molesky *et al.* [Opt. Express **21**, A96–A110 (2013)]. Here, we show how the long-standing search for a high temperature narrowband near-field emitter for thermophotovoltaics can be fulfilled by thermally exciting plasmons. We also describe a method to control Wein's displacement law in the near-field using high temperature epsilon-near-zero metamaterials. Finally, we show that our work opens up an interesting direction of research for the field of slow light: thermal emission control. © 2014 AIP Publishing LLC. [<http://dx.doi.org/10.1063/1.4893665>]

Nanoengineering the coherent state of light as in a SPASER¹ and the quantum state of light through plasmonic single photon sources² have received significant attention over the last few years. However, control over the thermal state of light for nanoscale thermal sources with spectral tuning, narrow bandwidth and spatial coherence remains a challenge. In this paper, our aim is to show that thermally exciting plasmons³ can lead to novel near-field thermal sources. This is a paradigm shift away from the conventional approaches of exciting bulk and surface plasmons through fast electrons,⁴ momentum matched light,^{5,6} or quantum emitters.⁷

One major application of such narrowband thermal sources with super-Planckian thermal emission can be in micron gap or near-field thermophotovoltaics.^{8–10} The conventional Shockley-Queisser limit of energy conversion only applies for a thermal source with the black-body spectrum.¹¹ As opposed to this, if the thermal emission is spectrally matched to the bandgap of the photovoltaic cell, the efficiency of conversion can exceed the Shockley Queisser limit.¹² One important condition on the thermal source for thermophotovoltaics is the wavelength of emission which has to be between $1\ \mu\text{m} < \lambda < 2\ \mu\text{m}$ ($T \approx 1200\ \text{K}$) for compatibility with low bandgap thermophotovoltaic cells. We note that significant advances have been made in the field of tungsten photonic crystals^{13–15} and metamaterials¹⁶ for thermal engineering^{17–19} but not narrowband high temperature near-field emission. On the other hand, surface-phonon-polariton (SPhP) approaches for tailoring near-field thermal emission which rely on natural material resonances (e.g., SiC in the mid-IR) are not tunable to the spectral ranges relevant to low bandgap photovoltaics.¹⁷

S. Molesky *et al.* introduced the concept of high temperature plasmonics and metamaterials for thermophotovoltaics.²⁰ Plasmon-polaritons are higher energy excitations than phonon-polaritons and thus can be tuned to the wavelength ranges compatible with thermophotovoltaic cells.

This approach required a switch away from conventional plasmonic building blocks like silver and gold to alternate plasmonic materials based on oxides and nitrides.^{21,22} Note, conventional metals with plasma frequency at ultraviolet frequencies have shown thermal plasmonic effects³ but would melt well before the black-body temperature is able to provide efficient emission for thermophotovoltaic applications. We emphasize that alternate plasmonic media can have high melting points in the range of $3000\ ^\circ\text{C}$ allowing operation in the near-IR range crucial for practical applications.

In this paper, we show that epsilon-near-zero²³ (ENZ) and surface-plasmon-polaritons (SPPs) resonances in anisotropic multilayer plasmonic metamaterials can lead to narrowband super-Planckian thermal emission in the near-field. We also show that plasmonic slow light modes^{24–26} behave like photonic van Hove singularities²⁷ which can lead to near-field thermal emission beyond the black-body limit. We further consider the potential application for near-field thermophotovoltaics where the narrowband thermal emission must be between $1\ \mu\text{m} < \lambda < 2\ \mu\text{m}$ for efficient energy conversion beyond the Shockley Queisser limit using low bandgap GaSb photovoltaic cells ($E_{\text{gap}} = 0.7\ \text{eV}$). We emphasize that neither photonic crystals nor surface phonon polaritons can show narrowband super-Planckian near-field thermal emission in the near-infrared wavelength ranges.

Throughout the paper we use Rytov's fluctuational electrodynamics²⁸ to calculate the near-field thermal properties. The near-field energy density near a planar interface or slab is given by²⁹

$$u(d, T) = \int_0^\infty d\lambda \frac{1}{2} u_0(\lambda, T) \sum_{j=s,p} \left\{ \int_0^1 \frac{k_\rho dk_\rho}{k_0 |k_z|} \frac{(1 - |r_j|^2)}{2} + \int_1^\infty \frac{k_\rho^3 dk_\rho}{|k_z| k_0^3} e^{-2\text{Im}(k_z)k_0 d} \text{Im}(r_j) \right\}, \quad (1)$$

where $u_0(\lambda, T) = 8\pi hc / (\lambda^5 (e^{hc/\lambda k_B T} - 1))$, T is the temperature of the body, d is the distance at which the energy density is measured, r_s and r_p are the reflection coefficients of (s)

^{a)}zjacob@ualberta.ca

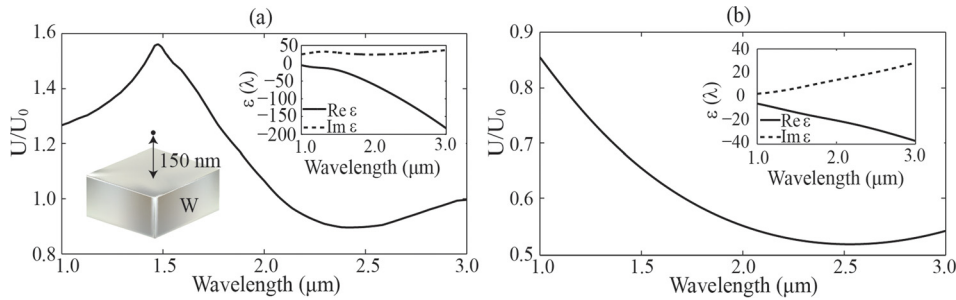


FIG. 1. (a) Near-field thermal emission normalized to the black-body emission (U_0) for a 500 nm tungsten slab; the observation distance is 150 nm. (b) Normalized near-field thermal emission for a 500 nm TiN slab; same observation distance. The dielectric constants are shown in the inset. Such broadband near-field sources are not suited for thermophotovoltaics.

and (p) polarized waves incident on the interface, k_ρ is the lateral wavevector, and k_z is the wavevector perpendicular to the interface (normalized to free space wavevector). We first consider the case of tungsten, a lossy metal with high temperature stability and analyze its near-field thermal emission (Fig. 1(a)). As is well known from Rytov's theory, any lossy medium possesses an enhanced non-radiative near-field local density of states $\rho^{n-rad}(d \ll \lambda) \approx \epsilon''/(4|\epsilon + 1|^2(k_0 d)^3)$ which is manifested in the near-field thermal energy density. This non-radiative enhancement can be attributed to the excitation of lossy surface waves³⁰ because such waves if incident on a surface are immediately absorbed. Note that high losses in the medium ($\epsilon'' \gg 1$) can lead to a spectrally broad thermal emission beyond the black-body limit, however, the effect is limited by the large absolute value of the dielectric constants $\rho^{n-rad}(d \ll \lambda) \propto 1/|\epsilon + 1|^2$. The goal therefore is to shift to metals with SPP resonance in the near-infrared range coupled with high temperature stability. In Fig. 1(b), we show the near-field thermal emission from titanium nitride, an alternate plasmonic metal²¹ whose high temperature properties for thermophotovoltaics were pointed out by Molesky *et al.*²⁰ We see that TiN does not show any enhancement compared to free-space energy density in the spectral range relevant to thermophotovoltaics (TPV) because the SPP resonance is located around 700 nm. The plasma frequency can be tuned by the deposition conditions however for recently reported values²¹ we see that the surface-plasmon-polariton peak cannot be efficiently excited at temperatures of 1000 K. The corresponding figure insets show the stark contrast in the dielectric constant values of tungsten and titanium nitride in the near-infrared range. The optical constants are given in the supplementary material.³¹ Tuning the plasma frequency of titanium nitride to the near-infrared ranges would make it an excellent candidate for thermophotovoltaic applications.

In contrast, aluminum doped zinc oxide (AZO) which has a plasma energy of 1.75 eV shows a better enhancement in the near-field thermal emission (Fig. 2(a)). Beyond the epsilon-near-zero wavelength ($\lambda_{ENZ} \approx 1437$ nm), thin AZO

films provide an enhancement in the near-field thermal emission. The thin film supports two coupled surface plasmon polaritons (short range and long range) which gives rise to peaks in thermal emission. The broad peak is related to the short range SPP and lossy surface wave contribution in the near-field of the thin film. This spectral behavior is not ideally suited for thermophotovoltaics. The goal of achieving a narrowband near-field thermal source can be achieved by using substrate effects to tune the SPP resonances. Fig. 2(b) shows the role of the substrate to tune the SPP resonance leading to a narrowband peak in thermal emission. Our analysis shows that the optimum solution for narrowband thermal sources consist of using simple thin films of a high temperature plasmonic material with low damping on an appropriately chosen substrate for tuning.

We now discuss another route of achieving a narrowband super-Planckian thermal source with tunability. Multilayer metal-dielectric metamaterials also support ENZ resonances and tunable anisotropic surface plasmon polariton resonances along with hyperbolic modes.³²⁻³⁴ Previous work has shown that hyperbolic dispersion leads to broadband super-Planckian thermal emission.^{35,36} Here, we report the narrow peak of thermal emission due to ENZ and anisotropic SPP modes of multilayer metamaterials with AZO and zinc oxide (ZnO) which can be spectrally tuned by varying the fill fraction (Fig. 3). From Fig. 3(a), it is seen that the super-Planckian thermal emission peak is tuned as the fill fraction is changed from $\rho = 1$ (thin metallic film) to $\rho = 0$ (thin dielectric film). The physical origin of the thermal emission peak is remarkably different for varying fill fractions and changes from isotropic surface waves to anisotropic surface waves and finally a bulk epsilon-near-zero mode at low fill fractions when $\rho < 0.5$. We emphasize that thermally activated nonlinearities in the dielectric constituent of the metamaterial can also lead to similar tuning of the epsilon-near-zero wavelength but solely through temperature effects. This thermal tuning effect will correspond to a generalization of Wein's displacement law to the near-field.

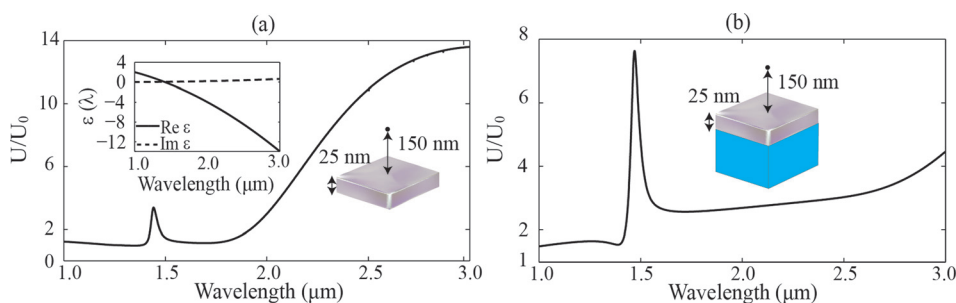


FIG. 2. (a) Normalized thermal emission for a 25 nm AZO slab; the observation distance is 150 nm. Coupled surface plasmons of thin films play a key role in the thermal emission. (b) Normalized thermal emission for a 25 nm AZO slab with a dielectric substrate ($\epsilon=6$), the distance is 150 nm. The substrate leads to tuning of the SPP resonance and a narrowband peak in the thermal emission.

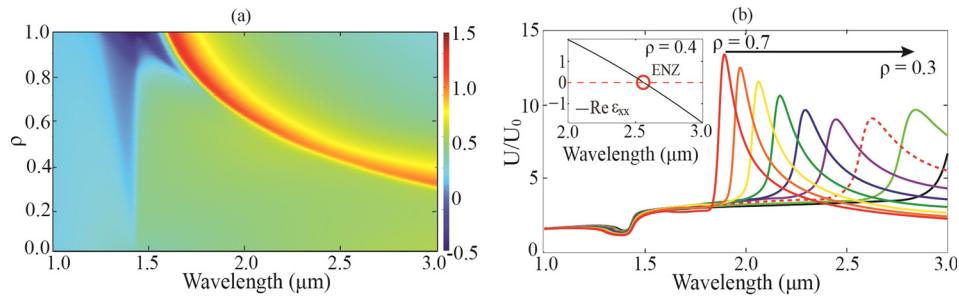


FIG. 3. (a) Near field thermal emission enhancement (log scale plot) due to epsilon-near-zero resonances and anisotropic surface plasmon polaritons of multilayer AZO/ZnO metamaterials; the observation distance is 150 nm from the multilayer metamaterial. The bright red band is the super-planckian thermal emission which can be tuned by changing the fill fraction. (b) Thermal emission spectrum for fill fractions ρ varying from 0.3 to 0.7. We can tune the thermal emission peaks over a wide spectral range using the fill fraction of metal in the metamaterial.

Away from the epsilon-near-zero region multilayer thin film metamaterials show unique spectral signatures in the near-field thermal emission. In Fig. 4, we consider a multilayer metal-dielectric structure consisting of AZO and ZnO with layer thicknesses of 25 nm each. They achieve an effectively anisotropic response with type I hyperbolic behavior between 1.43 μm and 2.25 μm and type II hyperbolic behavior beyond 2.25 μm . The thermal excitation of modes of this structure leads to multiple narrowband peaks in the near field (Fig. 4(a)). To understand the origin of the peaks, we plot the wavevector resolved local density of states²⁷ for the structure in Fig. 4(b). The bright bands correspond to the modes of the structure which are thermally excited. It is seen that the near-field thermal energy density peak occurs at the wavelength where the group velocity of the mode approaches zero.

This enhancement in the thermal emission and density of states is due to a photonic van Hove singularity (VHS)

that arises from the slow light modes in this coupled-plasmonic structure.²⁷ We argue that electronic equivalent of such thermal emission effects have been observed in lower dimensional systems like carbon nanotubes (CNTs). For example, current driven thermal emission from CNTs has shown unique spectral features corresponding to electronic VHS.^{37,38} Quantum confinement is necessary to observe the enhancement in the electronic density of states due to the integrable nature of the singularity in 3D. Our results shown in Fig. 4 are the photonic equivalent of such VHS based thermal phenomena. The tunneling of electrons measured using scanning tunneling microscopy (STM) also exhibits an enhancement at energies corresponding to van Hove singularities in the electronic density of states of carbon nanotubes.³⁴ The results of Fig. 4(a) can therefore be measured by the photonic equivalent of the STM experiment which is near-field thermal emission spectroscopy.^{29,39}

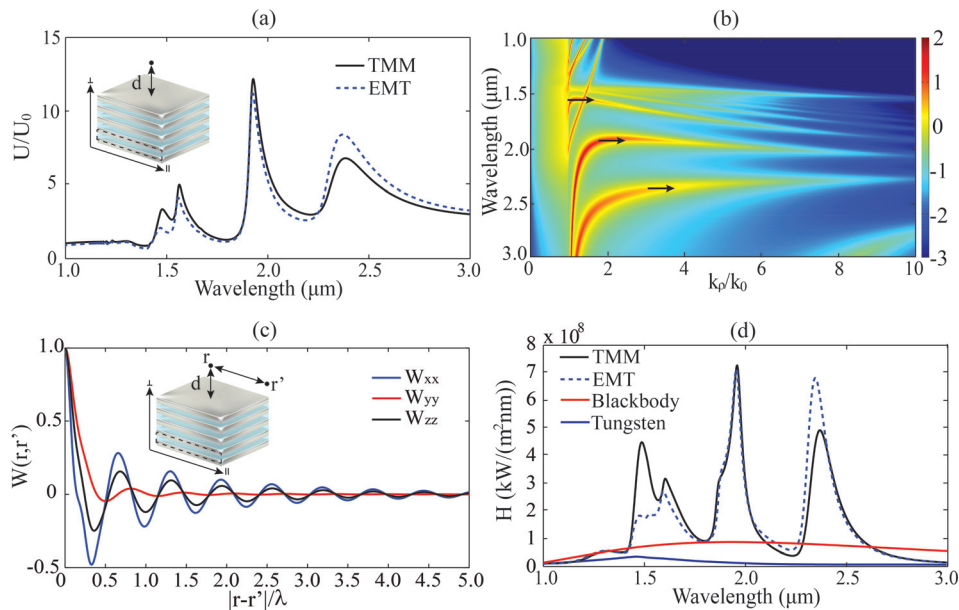


FIG. 4. (a) Near-field thermal emission peaks due to slow light modes in AZO/ZnO multilayer hyperbolic metamaterials. These peaks arise due to photonic van Hove singularities where the density of states and thermal emission are enhanced. We have taken into account loss, dispersion, finite unit cell, and finite sample size in our calculations. (Parameters: AZO and ZnO ($\epsilon = 6$) multilayers, each layer 25 nm and 20 layers in total, the observation distance is 150 nm.) (b) Wave-vector resolved thermal emission. The bright bands denote the modes of the structure which are thermally excited. We can clearly see slow light modes corresponding to the thermal emission peaks where the slope of the band goes to zero. (c) Spatial coherence at the spectral location of the second slow light mode (1927 nm). Note that the thermal excitation of the slow light mode (coupled-plasmonic state) gives rise to spatial coherence in the near field. (d) Spectrally resolved near-field heat transfer between two identical multilayers with a gap of 150 nm, $T_1 = 1500$ K, and $T_2 = 300$ K. The black-body heat transfer is shown for comparison. The slow light modes leads to super-Planckian heat transfer and there is an excellent correspondence between the results of effective medium theory and the practical multilayer structures.

Along with narrowband operation, another figure of merit of thermal sources is related to the spatial coherence.⁴⁰ Black-body thermal emission is spatially incoherent as signified by the Lambertian radiation pattern in the far-field. The presence of gratings,^{41,42} photonic crystals,⁴³ or epsilon-near-zero materials²⁰ has been shown to produce thermal antenna effects, i.e., spatial coherence in far-field thermal radiation. In the case of near-field thermal emission, the excitation of surface waves can lead to high degree of spatial coherence.⁴⁰ In Fig. 4(c), we analyze the near-field spatial coherence of our narrowband tunable thermal source arising from photonic van Hove singularities. We note that these are not surface states of the slab but bulk waveguide modes. The spatial coherence is determined by the spectral density tensor $W_{ij}(r, r', \omega)$ which characterizes the correlation of the electromagnetic fields as a function of distance.⁴⁴ We see an excellent spatial coherence

along the direction parallel to the planar interface due to the preferential thermal excitation of the slow light waveguide mode. The existence of spatial coherence is discerned by the oscillatory nature of the field correlations as opposed to their exponentially decaying behavior expected from incoherent thermal emission from a black-body. Similar effects are also expected for the anisotropic surface plasmon polariton waves.

A pertinent issue is the optimum design which achieves maximum heat transfer.⁴⁵ We emphasize that the simple thin film design presented in Fig. 2 which tunes the surface plasmon polaritons using substrate effects forms a promising solution. However, depending on the temperature of operation, spectral operating range and material properties there can be exceptions. We calculate the near-field heat transfer⁴⁶ between thin film nanostructures at temperatures T_1 and T_2 separated by a gap d

$$H(d, T_1, T_2) = \int_0^\infty d\lambda (H_0(\lambda, T_1) - H_0(\lambda, T_2)) \sum_{j=s,p} \left\{ \int_0^1 k_\rho dk_\rho \frac{(1 - |r_j^{01}|^2)(1 - |r_j^{02}|^2)}{|1 - r_j^{01} r_j^{02} e^{2ik_z k_0 d}|^2} + \int_1^\infty k_\rho dk_\rho e^{-2\text{Im}(k_z)k_0 d} \frac{4\text{Im}(r_j^{01})\text{Im}(r_j^{02})}{|1 - r_j^{01} r_j^{02} e^{2ik_z k_0 d}|^2} \right\}, \quad (2)$$

where $H_0(\lambda, T) = 2\pi hc^2 / (\lambda^5 (e^{hc/\lambda k_B T} - 1))$ and all other terms are defined similar to the near-field energy density. The result of this figure clearly shows that the near field heat transfer for our multilayer structures supporting the van Hove singularity can far exceed the value in tungsten. In Fig. 4(d), we plot the heat transfer between multilayer AZO/ZnO structures. The temperature of the two slabs are taken to be $T_1 = 1500$ K and $T_2 = 300$ K. We note the excellent agreement between effective medium predictions (EMT) of the location of the van Hove singularity and the practical multilayer structure (Transfer matrix method—TMM).

In conclusion, we have suggested a paradigm shift for plasmonics: thermal excitation. We have analyzed the potential of high temperature plasmonic metamaterials as narrowband tunable thermal sources for applications in thermophotovoltaics and near-field thermal stamping. Currently, material losses are a major impediment but future improvements in deposition techniques and optimization can lead to practical sources. Our work also paves the way for manipulating the near-field spatial coherence and bandwidth of thermal sources using metamaterials.

This work was partially supported by funding from Helmholtz Alberta Initiative, Alberta Innovates Technology Futures, and National Science and Engineering Research Council of Canada.

¹D. J. Bergman and M. I. Stockman, *Phys. Rev. Lett.* **90**, 27402 (2003).

²D. Chang, A. Sorensen, P. Hemmer, and M. Lukin, *Phys. Rev. Lett.* **97**, 53002 (2006).

³M. Kreiter, J. Oster, R. Sambles, S. Herminghaus, S. Mittler-Neher, and W. Knoll, *Opt. Commun.* **168**, 117 (1999).

⁴H. Raether, *Springer Tracts Modern Physics* (Springer Berlin Heidelberg, 1965), Vol. 38, pp. 84–157.

⁵E. Kretschmann and H. Raether, *Z. Naturforsch., A* **23**, 2135 (1968).

⁶A. Otto, *Z. Phys.* **216**, 398 (1968).

⁷A. Akimov, A. Mukherjee, C. Yu, D. Chang, A. Zibrov, P. Hemmer, H. Park, and M. Lukin, *Nature* **450**, 402 (2007).

⁸A. Narayanaswamy and G. Chen, *Appl. Phys. Lett.* **82**, 3544 (2003).

⁹M. Laroche, R. Carminati, and J.-J. Greffet, *J. Appl. Phys.* **100**, 063704 (2006).

¹⁰S. Basu, Z. M. Zhang, and C. J. Fu, *Int. J. Energy Res.* **33**, 1203 (2009).

¹¹W. Shockley and H. J. Queisser, *J. Appl. Phys.* **32**, 510 (1961).

¹²E. Rephaeli and S. Fan, *Opt. Express* **17**, 15145 (2009).

¹³S.-Y. Lin, J. Moreno, and J. G. Fleming, *Appl. Phys. Lett.* **83**, 380 (2003).

¹⁴I. Celanovic, N. Jovanovic, and J. Kassakian, *Appl. Phys. Lett.* **92**, 193101 (2008).

¹⁵V. Rinnerbauer, S. Ndao, Y. X. Yeng, W. R. Chan, J. J. Senkevich, J. D. Joannopoulos, M. Soljačić, and I. Celanovic, *Energy Environ. Sci.* **5**, 8815 (2012).

¹⁶X. Liu, T. Tyler, T. Starr, A. F. Starr, N. M. Jokerst, and W. J. Padilla, *Phys. Rev. Lett.* **107**, 045901 (2011).

¹⁷X. L. Liu, T. J. Bright, and Z. M. Zhang, *J. Heat Transfer* **136**, 092703 (2014).

¹⁸X. L. Liu, R. Z. Zhang, and Z. M. Zhang, *Appl. Phys. Lett.* **103**, 213102 (2013).

¹⁹J. J. Greffet, R. Carminati, K. Joulain, J. P. Mulet, S. Mainguy, and Y. Chen, *Nature* **416**, 61 (2002).

²⁰S. Molesky, C. J. Dewalt, and Z. Jacob, *Opt. Express* **21**, A96–A110 (2013).

²¹G. V. Naik, J. Kim, and A. Boltasseva, *Opt. Mater. Express* **1**, 1090 (2011).

²²G. V. Naik and A. Boltasseva, *Phys. Status Solidi RRL* **4**, 295 (2010).

²³A. Alù, M. G. Silveirinha, A. Salandrino, and N. Engheta, *Phys. Rev. B* **75**, 155410 (2007).

²⁴L. V. Alekseyev and E. Narimanov, *Opt. Express* **14**, 11184 (2006).

²⁵K. L. Tsakmakidis and O. Hess, *Phys. B: Condens. Matter* **407**, 4066 (2012).

²⁶P. Yao, C. Van Vlack, A. Reza, M. Patterson, M. M. Dignam, and S. Hughes, *Phys. Rev. B* **80**, 195106 (2009).

²⁷C. L. Cortes and Z. Jacob, *Phys. Rev. B* **88**, 045407 (2013).

²⁸S. M. Rytov, Y. A. Kravtsov, and V. I. Tatarskii, *Principles of Statistical Radiophysics 3* (Springer-Verlag, Berlin, 1989).

²⁹K. Joulain, R. Carminati, J. P. Mulet, and J. J. Greffet, *Phys. Rev. B* **68**, 245405 (2003).

- ³⁰G. Ford and W. Weber, *Phys. Rep.* **113**, 195 (1984).
- ³¹See supplementary material at <http://dx.doi.org/10.1063/1.4893665> for details.
- ³²C. L. Cortes, W. Newman, S. Molesky, and Z. Jacob, *J. Opt.* **14**, 063001 (2012).
- ³³D. R. Smith, D. Schurig, J. J. Mock, P. Kolinko, and P. Rye, *Appl. Phys. Lett.* **84**, 2244 (2004).
- ³⁴V. A. Podolskiy and E. E. Narimanov, *Phys. Rev. B* **71**, 201101 (2005).
- ³⁵S.-A. Biehs, M. Tschikin, and P. Ben-Abdallah, *Phys. Rev. Lett.* **109**, 104301 (2012).
- ³⁶Y. Guo, C. L. Cortes, S. Molesky, and Z. Jacob, *Appl. Phys. Lett.* **101**, 131106 (2012).
- ³⁷D. Mann, Y. K. Kato, A. Kinkhabwala, E. Pop, J. Cao, X. Wang, L. Zhang, Q. Wang, J. Guo, and H. Dai, *Nat. Nanotechnol.* **2**, 33 (2007).
- ³⁸P. Kim, T. W. Odom, J.-L. Huang, and C. M. Lieber, *Phys. Rev. Lett.* **82**, 1225 (1999).
- ³⁹A. C. Jones and M. B. Raschke, *Nano Lett.* **12**, 1475 (2012).
- ⁴⁰Z. Zhang, *Nano/Microscale Heat Transfer*, 1st ed. (McGraw-Hill Professional, 2007).
- ⁴¹J. A. Mason, D. C. Adams, Z. Johnson, S. Smith, A. W. Davis, and D. Wasserman, *Opt. Express* **18**, 25192 (2010).
- ⁴²B. J. Lee, L. P. Wang, and Z. M. Zhang, *Opt. Express* **16**, 11328 (2008).
- ⁴³M. Laroche, R. Carminati, and J. J. Greffet, *Phys. Rev. Lett.* **96**, 123903 (2006).
- ⁴⁴R. Carminati and J. J. Greffet, *Phys. Rev. Lett.* **82**, 1660 (1999).
- ⁴⁵O. D. Miller, S. G. Johnson, and A. W. Rodriguez, *Phys. Rev. Lett.* **112**, 157402 (2014).
- ⁴⁶S. Shen, A. Narayanaswamy, and G. Chen, *Nano Lett.* **9**, 2909 (2009).